Matricellular Protein SPARCL1 Regulates Blood Vessel Integrity and Antagonizes Inflammatory Bowel Disease

Daniela Regensburger, MSc,[*] Clara Tenkerian, PhD,[*] Victoria Pürzer, MSc, Benjamin Schmid, PhD,[†] Thomas Wohlfahrt, PhD,[‡] Iris Stolzer, MSc,[§] Rocío López-Posadas, PhD,[§] Claudia Günther, PhD,[§] Maximilian J. Waldner, MD,[§] Christoph Becker, PhD,[§] Heinrich Sticht, PhD,[¶] Katja Petter, MSc,[*] Christian Flierl,[*] Tobias Gass,[*] Tim Thoenissen,[*] Carol I. Geppert, MD,[‖] Nathalie Britzen-Laurent, PhD,[*] Valérie S. Méniel, PhD,[**] Andreas Ramming, MD,[‡] Michael Stürzl, PhD,[,a] and Elisabeth Naschberger, PhD[*,a]*

Background: The understanding of vascular plasticity is key to defining the role of blood vessels in physiologic and pathogenic processes. In the present study, the impact of the vascular quiescence marker SPARCL1 on angiogenesis, capillary morphogenesis, and vessel integrity was evaluated.

Methods: Angiogenesis was studied using the metatarsal test, an ex vivo model of sprouting angiogenesis. In addition, acute and chronic dextran sodium sulfate colitis models with SPARCL1 knockout mice were applied.

Results: This approach indicated that SPARCL1 inhibits angiogenesis and supports vessel morphogenesis and integrity. Evidence was provided that SPARCL1-mediated stabilization of vessel integrity counteracts vessel permeability and inflammation in acute and chronic dextran sodium sulfate colitis models. Structure-function analyses of purified SPARCL1 identified the acidic domain of the protein necessary for its anti-angiogenic activity.

Conclusions: Our findings inaugurate SPARCL1 as a blood vessel–derived anti-angiogenic molecule required for vessel morphogenesis and integrity. SPARCL1 opens new perspectives as a vascular marker of susceptibility to colitis and as a therapeutic molecule to support blood vessel stability in this disease.

Key Words: angiogenesis, blood vessel, DSS colitis, endothelial cell, inflammatory bowel disease, permeability, SPARCL1

INTRODUCTION

Blood vessels establish a structural and functional component in all major diseases including cardiovascular diseases, cancer, and inflammation. The view on the role of blood vessels in physiologic processes and diseases is changing significantly. Until recently, blood vessels were considered as stable tubular structures, solely dedicated to transporting oxygen and nutrients. Now it has become apparent that they establish a highly dynamic organ-like structure, with manifold interactions with their microenvironment and significant involvement in the regulation of physiologic processes and diseases.[1]

This new concept is based on the plasticity of blood vessels and their key structural components: endothelial cells, which form the inner layer of the vessel, and pericytes, which exert stabilizing functions and counteract vessel permeability.[2] Modern molecular analyses have shown that endothelial cells in

Received for publications December 10, 2020; Editorial Decision December 15, 2020.

From the *Division of Molecular and Experimental Surgery, Translational Research Center, Department of Surgery, University Medical Center Erlangen, Friedrich-Alexander Universität Erlangen-Nürnberg, Erlangen, Germany; †Optical Imaging Centre, Friedrich-Alexander Universität Erlangen-Nürnberg, Erlangen, Germany; ‡Department of Internal Medicine 3, Rheumatology and Immunology, University Medical Center Erlangen, Friedrich-Alexander Universität Erlangen-Nürnberg, Erlangen, Germany; §Department of Medicine 1, Gastroenterology, Pneumology and Endocrinology, University Medical Center Erlangen, Friedrich-Alexander Universität Erlangen-Nürnberg, Erlangen, Germany; ¶Division of Bioinformatics, Institute of Biochemistry, Friedrich-Alexander Universität Erlangen-Nürnberg, Erlangen, Germany; ‖Institute of Pathology, University Medical Center Erlangen, Friedrich-Alexander Universität Erlangen-Nürnberg, Erlangen, Germany; **European Cancer Stem Cell Research Institute, Cardiff University, Cardiff, United Kingdom

[a]These authors jointly supervised this work.

Author contributions: DR, EN, and MS designed the experiments. CF, CT, DR, KP, TG, TT, VP, and EN performed the experiments. BS, CT, DR, EN, HS, CIG, and MS analyzed the data. AR, BS, CB, CG, IS, MJW, NBL, RLP, TW, and VSM provided key reagents, materials, analysis tools, and helpful ideas. DR, EN, and MS: wrote the manuscript. All authors approved the final version of the manuscript.

Supported by: This work was supported by the German Research Foundation grants FOR 2438 (subproject 2 to EN and MS), SFB/TRR 241 (subproject A06 to MS and NBL), and STU 238/10–1 (to MS); the Interdisziplinäres Zentrum für Klinische Forschung Erlangen (D28, D34, and J73 to EN, AR, MS, and CT); the W. Lutz Stiftung (to MS); and the Forschungsstiftung Medizin am Universitätsklinikum Erlangen (to MS). Address correspondence to: Elisabeth Naschberger, PhD, Division of Molecular and Experimental Surgery, Translational Research Center, Department of Surgery, University Medical Center Erlangen, Friedrich-Alexander Universität Erlangen-Nürnberg, Erlangen, Germany (elisabeth.naschberger@uk-erlangen.de).

doi: 10.1093/ibd/izaa346
Published online 4 January 2021

normal and diseased tissues exhibit heterogeneous phenotypes.[1, 3] This notion was based on studies with molecular markers that can distinguish endothelial cells originating from different types of vessels (eg, arterial [ephrin-B2], venous [Eph-B4], and lymphatic [podoplanin]),[4-6] different organs,[7, 8] diseased vs healthy tissues (tumor vessel markers in the colon),[9] and different stages during angiogenesis (stalk cell [Tie 2], tip cell [Esm-1]).[10-12] Significant heterogeneity of endothelial cells has been detected in tumor tissues and has been found to change in dependence on the specific tumor microenvironments (TME).[1, 3] It is likely that the different molecular markers of endothelial cell heterogeneity will also regulate endothelial cell plasticity and may provide specific targets of vessel-directed therapy. However, the specific functions of these markers are often unclear.

Recently, the secreted protein, acidic and rich in cysteine-like 1 (human: SPARCL1/hevin; murine: Sc1) has been identified as characterizing tumor vessels in colorectal carcinoma (CRC) tissues with a specific tumor microenvironment.[3] SPARCL1 is a member of the SPARC family of secreted matricellular proteins, together with SPARC/osteonectin, SPARC-related modular calcium-binding proteins (SMOCs), testicans, and follistatin-like protein 1.[13] SPARC/osteonectin and SPARCL1/hevin/Sc1 are closely related at the structural level.[14] They are composed of an N-terminal signal peptide causing secretion of the proteins, an internal follistatin-like domain (FLD), and a C-terminal extracellular calcium-binding domain (ECBD). Both proteins differ in their highly acidic domain (AD), which is positioned between the signal peptide sequence and the FLD and is 411 amino acids long in SPARCL1 but only 51 amino acids long in SPARC.[14]

SPARCL1 has been highly expressed in tumor vessel endothelial cells from CRC with a favorable prognosis and has been downregulated in the tumor vessel endothelial cells of aggressive CRC.[3] A CRC with favorable prognosis has exhibited an interferon-γ-dominated angiostatic Th1-like TME and was characterized by vessels with a more mature phenotype and higher pericyte coverage.[3, 15] SPARCL1 has not been detected in proliferating endothelial cells, but its expression was highly induced in quiescent endothelial cells, both in cell culture and in tissues.[3] Notably, endothelial SPARCL1 has been secreted and has inhibited the proliferation of endothelial cells[3] and of different cancer cell lines[16] in culture. These results indicate that SPARCL1 is a vessel-derived angiocrine factor that stabilizes blood vessels in homeostasis and in addition counteracts tumor growth in CRC with a prognostically favorable TME.

The vessel-stabilizing function of SPARCL1 may also be of relevance for inflammatory bowel diseases (IBD), another prominent disease of the colon. Recently, it has been shown that a dysfunction of the vascular barrier is an important pathomechanism in IBD.[17, 18] The IBD-associated cytokine interferon-γ caused a breakdown of the vascular barrier in one study through disruption of the adherens junction protein VE-cadherin, and this was found as a crucial driver of dextran sodium sulfate (DSS)-induced experimental colitis. These results were also confirmed in human patients with IBD.[18]

The understanding of vascular plasticity is key to defining the role of blood vessels in physiologic and pathogenic processes. In the present study, the impact of the quiescence marker SPARCL1 on angiogenesis, capillary morphogenesis, and vessel integrity in vitro was evaluated using the metatarsal test. This test in comparison with other commonly used angiogenesis assays provides a more representative model of sprouting angiogensis in vivo.[19] It revealed that SPARCL1 inhibits angiogenesis and regulates vessel morphogenesis and integrity. In addition, we provide evidence that the stabilizing effect of SPARCL1 on vessel integrity may be of clinical relevance in IBD, and we identified the structural domain required for SPARCL1 anti-angiogenic activity. Our findings inaugurate SPARCL1 as a novel angiocrine regulatory molecule of vessel stability with clinical relevance for IBD.

MATERIALS AND METHODS

Immunofluorescence Analysis

For immunofluorescence analyses, hindlimbs from Sc1 wild-type (WT) C57BL/6 E18.5 mice were used. Tissues were processed as described previously.[3, 18] Antigen retrieval was accomplished using target retrieval solution, pH 9.0 (DakoCytomation/Agilent, Frankfurt, Germany.). Goat anti-mouse SPARCL1 antibody (1:50, catalog no. AF2836, R&D Systems, Minneapolis, MN), rat anti-mouse CD31 (1:100, clone SZ31, catalog no. DIA-310, Dianova, Hamburg, Germany), and rabbit anti-mouse smooth muscle actin (1:1000, catalog no. ab124964, Abcam, Cambridge, UK) were used as primary antibodies and incubated for 1 hour at room temperature. As controls, the following isotype antibodies were used with the same final concentrations and incubation time as the respective detection antibody: rat IgG2a (clone 54447, R&D Systems, Minneapolis, MN), goat IgG (catalog no. AB-108-C, R&D Systems, Minneapolis, MN), and rabbit IgG (catalog no. AB-105-C, R&D Systems, Minneapolis, MN). AF546-conjugated donkey anti-rabbit (1:500, catalog no. A-10040, Thermo Fisher Scientific, Waltham, MA), AF488-conjugated donkey anti-goat (1:500, catalog no. A-11055, Thermo Fisher Scientific, Waltham, MA), and AF555-conjugated donkey anti-rat (1:500, catalog no. 6430–32, Southern Biotech, Birmingham, AL) were used as secondary antibodies and incubated for 45 minutes at room temperature. The slides were then incubated with Draq5 [1, 5-bis{[2-(di-methylamino)ethyl] amino}-4, 8-dihydroxyanthracene-9, 10-dione] (1:800, catalog no. 4084L, Cell Signaling Technology, Danvers, MA) for 10 minutes and mounted with fluorescence mounting medium (DakoCytomation, Santa Clara, CA). Pictures were taken using a laser-scanning confocal microscope (TCS SPE, Leica Microsystems, LAS-X software, Wetzlar, Germany).

Metatarsal Assay

Metatarsal bones were isolated from Sc1 knockout (Sc1 ko) and WT E18.5 embryos and cultured, stimulated, and stained as described in Song et al.[19] For cultivation, alphaMEM (catalog no. 32561-037, Thermo Fisher Scientific, Waltham, MA) with 10% fetal calf serum was used as the basal medium. On day 1, metatarsals were isolated and seeded. On days 3, 5, 7, and 9, bones were stimulated. The following recombinant proteins were used for stimulation: recombinant mouse SPARCL1 (1.5 µg/mL; catalog no. 4547-SL, R&D Systems, Minneapolis, MN), recombinant mouse VEGF-A (100 ng/mL; catalog no. 12343665, ImmunoTools, Friesoythe, Germany), and self-made recombinant human SPARCL1 (1.5 µg/mL) and human SPARCL1 mutants. For SPARCL1 neutralization, a goat anti-human SPARCL1 antibody (catalog no. AF2728, R&D Systems, Minneapolis, MN) and a goat IgG isotype antibody as a control (catalog no. AB-108-C, R&D Systems, Minneapolis, MN) were used in 5-fold molar excess concentrations compared to the recombinant human SPARCL1. On day 11, bones were fixed with 10% formalin (neutral buffered, Sigma Aldrich, Taufkirchen, Germany) and stained with the following primary antibodies (overnight at 4°C): rat anti-mouse CD31 (1:400, clone SZ31, catalog no. DIA-310, Dianova, Hamburg, Germany) and Sm22α (1:100, catalog no. ab10135, Abcam, Cambridge, UK). AF488-conjugated donkey anti-rat (1:500, catalog no. A-21208, Thermo Fisher Scientific, Waltham, MA) and AF546-conjugated donkey anti-goat (1:500, catalog no. A-11056, Thermo Fisher Scientific, Waltham, MA) were used as secondary antibodies and incubated for 2 hours at room temperature. Pictures were obtained using the tile-scan mode via a laser-scanning confocal microscope (TCS SPE, Leica Microsystems, LAS-X software, Wetzlar, Germany). Quantifications were performed using Fiji/ImageJ.[20] To analyze the number of branches and junctions, vessels were marked via tubeness (sigma = 5) and 3-dimensional hysteresis thresholding. Then the skeletonized picture was analyzed and the number of branches or junctions was summed up.

Cloning and Purification of Human SPARCL1/-Mutants

The respective cDNA fragments were cloned into the pMCV2.2 vector and expressed under control of the cytomegalovirus (CMV) promoter.[21] For detection and purification of SPARCL1 proteins, a C-terminal Flag-Glycine(9)-His-Tag was added. To obtain the different SPARCL1 mutants, the following parts of human WT SPARCL1 (National Center for Biotechnology Information reference: NP_001121782.1) were deleted: ΔAD: D26-V430; ΔFLD: C433-C509; ΔECBD: from C515 onward. The boundaries of the respective domains were set according to Girard and Springer[14] and additional bioinformatic analysis: the domain boundaries of FLD and ECBD were derived from the crystal structure of the homologous SPARC protein [protein data bank (PDB) code: 1BMO].[22] Finally, AD covered the remaining N-terminal part of SPARCL1, for which no 3-dimensional structural information was available.

The respective plasmids were transfected into HeLa cells using calcium phosphate precipitation.[23] Eight hours after transfection, the cells were cultured for 3 days with Opti-MEM Reduced Serum Medium (catalog no. 31985-047, Thermo Fisher Scientific, Waltham, MA). Next, the supernatants were harvested, protease inhibitors (cOmplete, EDTA-free protease inhibitor cocktail, catalog no. 4693132001, Roche, Basel, Switzerland) were added, and the proteins were purified from supernatants via His-Tag chromatography using the fast protein liquid chromatography (FPLC) Äkta system (GE Healthcare, Chicago, IL).[24] To prove the purity of the purified proteins, Coomassie staining of gels (SimplyBlue SafeStain, catalog no. LC6060, Thermo Fisher Scientific, Waltham, MA) and mass spectrometry (data not shown) were used. In the Coomassie gel, only the band of the purified protein was visible and mass spectrometry confirmed that the purified protein was the major product. Human WT SPARCL1, ΔFLD, and ΔECBD were quantified using the human SPARC-like 1/SPARCL1 DuoSet enzyme-linked immunosorbent assay (catalog no. DY2728, R&D Systems, Minneapolis, MN).[3] Because of the lack of antigens, the ΔAD could not be detected in this system and was therefore quantified by comparison to concentration curves of body surface area in gels after Coomassie staining and subsequent ImageJ analysis. Then the molecular weights of the proteins were calculated and subsequently confirmed by polyacrylamide gel electrophoresis and Coomassie staining, and equal molar concentrations of all purified proteins were calculated and used subsequently in the metatarsal assay.

Transgenic Mice

Female Sc1 ko C57BL/6 mice were used as described previously.[3, 18] Mice exhibited a complete ko by replacement of exon 2 in the *SPARCL1* gene by a Neo selection cassette, which leads to an out-of-frame gene disruption.[25] The mice from the different experimental groups were co-housed during all experiments. All animal studies were performed in accordance with German law and approved by the Institutional Animal Care and Use Committee of the University of Erlangen and the Animal Experiment Committee of the State Government of Lower Franconia, Würzburg, Germany.

In Vivo Permeability of Colonic Vessels

The experiment was performed and analyzed as described previously.[17, 18] Fluorescein isothiocyanate (FITC)-dextran (10 mg/mL; catalog no. FD70, Sigma Aldrich, Taufkirchen, Germany) and Alexa647-labeled lectin from *Bandeiraea simplicifolia* (100 µg/mouse in phosphate-buffered saline; catalog no. L2380, Sigma Aldrich, Taufkirchen, Germany) were injected intravenously. Colon vessel permeability was visualized

via a laser-scanning confocal microscope (TCS SPE, Leica Microsystems, LAS-X software, Wetzlar, Germany).

Induction and Evaluation of Acute and Chronic DSS-Induced Colitis

Acute colitis

The DSS (1.5%, 40 kDa; catalog no. 160110, Santa Ana, CA) was applied to the drinking water every second day for a total of 7 days, followed by 3 days of normal drinking water. Endoscopy, vessel permeability measurement, and endpoint harvest was conducted at day 9 or 10 (dependent on weight loss).

Chronic colitis

The DSS treatment was applied in a reduced concentration (1%) compared to the acute model in 3 repetitive cycles (7 days DSS, 14 days drinking water = 21 days each cycle). Endoscopy was conducted at day 10 after cycle 1 and at day 31 after cycle 2. Endoscopy after the third cycle was conducted at day 53. Vessel permeability measurement and endpoint harvest were conducted at day 55 (Fig. 3A).

Evaluation

To determine the grade of colitis, high-resolution mini-endoscopy was performed and evaluated as described in Langer et al.[18] The in vivo permeability of colonic vessels was analyzed, and mice were killed by cervical dislocation at the endpoint. To measure the colon length, colons were isolated from mice as described previously.[18] Hematoxylin-eosin stains of the colon were evaluated by a pathologist in a blinded manner. Sections were scored for the grade of inflammation with the following grades: 0 = negative, 1 = low, 2 = intermediate, and 3 = high.

Statistical Analysis

The χ^2 test was used to compare the sampling distribution. For all other analyses, the 2-tailed Student *t* test was performed. A P value < 0.05 was considered to be statistically significant. Calculations were carried out using SPSS (version 24, IBM Corp.) for the χ^2 test and GraphPad Prism (version 7, GraphPad Software) for the Student *t* test.

RESULTS

SPARCL1 Inhibits Angiogenesis

To investigate the impact of SPARCL1 on angiogenesis, the murine metatarsal sprouting assay was used.[19] For this assay, metatarsal bones from embryos of WT mice were isolated at gestational day 18.5 and put in culture. Under appropriate stimulation, this led to the formation of complex vessels covered by mural cells, which allowed the analysis of vessel sprouting, morphogenesis, and maturation (Supplementary Fig. 1). Costaining of SPARCL1 with the endothelial cell–associated marker CD31 and the pericyte marker αSMA, respectively, in tissues of the extremities of embryos of the WT mice showed that SPARCL1 is expressed in a vessel-associated manner in the metatarsals (Fig. 1A). Stainings with the isotypic control antibodies did not show any signals (Fig. 1A). Treatment of isolated metatarsals in culture with vascular endothelial growth factor-A resulted in increased vessel sprouting, which was significantly repressed when SPARCL1 was simultaneously present (Fig. 1B).

SPARCL1 Is Required for Capillary Morphogenesis and Integrity

To investigate the impact of SPARCL1 on vessel formation, metatarsals derived from Sc1 ko mice and WT mice were compared (Fig. 2A). In the absence of SPARCL1, the vessel morphology was highly disturbed, specifically in areas close to the bones. Vessels were dilated and the tubular morphology characteristically observed in vessels sprouting from the metatarsals of WT mice was lost (Fig. 2A). The significant morphologic alteration of vessels from Sc1 ko metatarsals in regions near the bone was confirmed at the quantitative level. Toward this goal, the metatarsal bones were outlined manually and the surrounding area traversed by the vessels was divided into 20 increments of equal area. For each increment, the ratio of the area covered by vessels (Fig. 2A, upper right) and, vice versa, the endothelial cell–free areas (Fig. 2A, lower right) compared to the total area were measured, using metatarsals from both WT and Sc1 ko mice. Both approaches confirmed that the intervascular cell–free area is significantly reduced in experiments with metatarsals from Sc1 ko mice, specifically in increments directly adjacent to the bones. Notably, the maximal distance from the bone reached by the complete vascular network was similar to that of the metatarsals from the Sc1 ko and WT mice. These results indicated that SPARCL1 is required for the formation of a normal vessel structure.

A recent study reported that disturbed vessel structure can be associated with increased permeability of vessels in the colon.[17, 18] Therefore, the impact of SPARCL1 on vessel permeability was investigated by intravital imaging of the vessels in colon crypts. The intestinal vasculature was visualized by the detection of 70 kDa FITC-dextran injected intravenously into Sc1 ko and WT mice. The accumulation of FITC-dextran in the lumen of the intestinal crypts of Sc1 ko mice indicated an increased vessel permeability as compared with those of WT mice (Fig. 2B). Increased permeability was also quantitatively analyzed by counting the relative numbers of leaky and nonleaky (healthy) crypts in WT and Sc1 ko mice. This approach showed that in the absence of SPARCL1, vessel permeability is significantly increased (Fig. 2B, right).

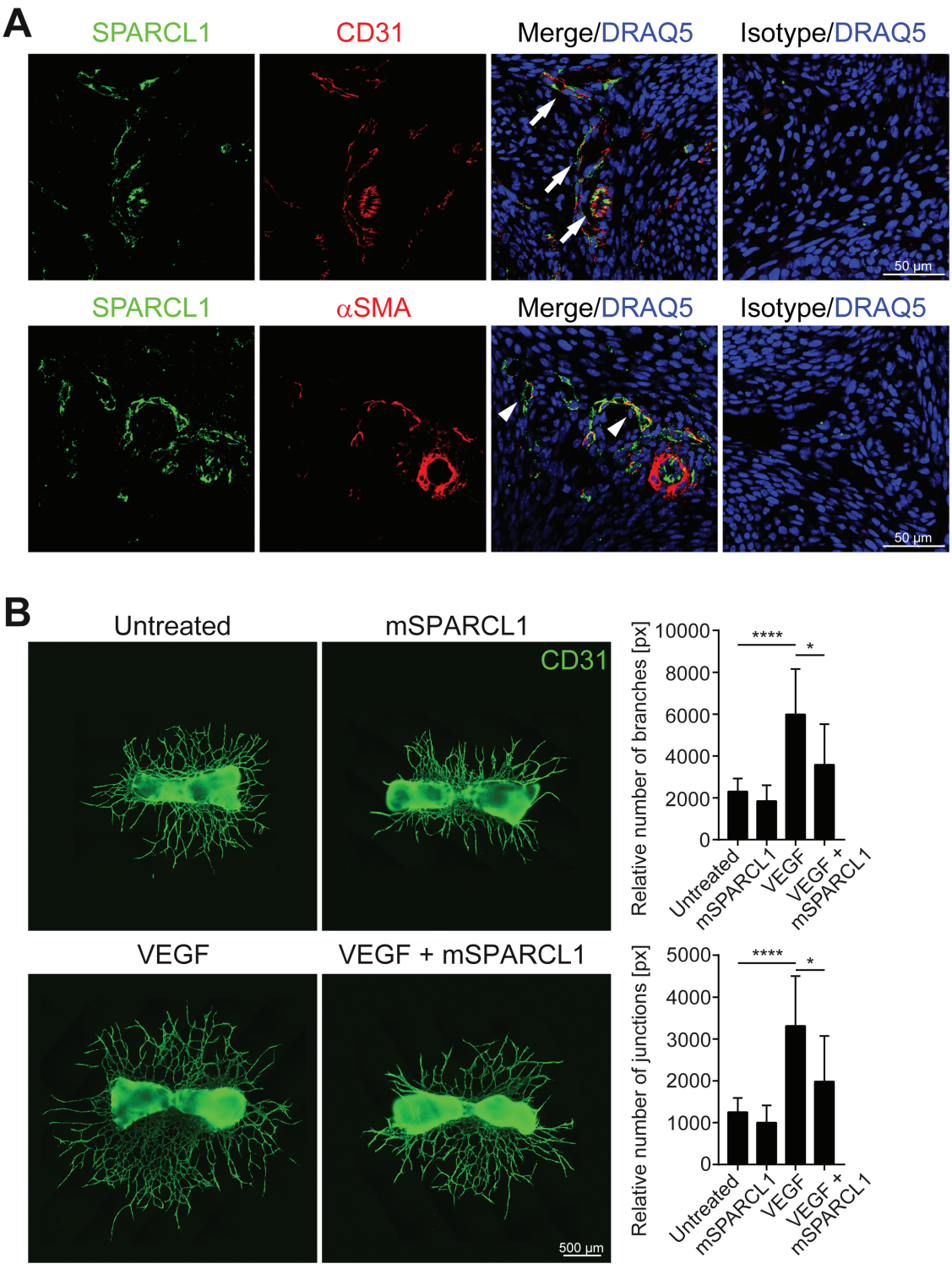

FIGURE 1. SPARCL1 is expressed in blood vessels of metatarsals and inhibits angiogenesis ex vivo. A, Tissues covering metatarsals of WT embryos at E18.5 (n = 4) were stained for SPARCL1 (green), CD31 (red, upper), and αSMA (red, lower). Examples of co-localization of SPARCL1 and CD31 indicated by arrows and examples of co-localization of SPARCL1 and αSMA indicated by arrowheads. Draq5 [1, 5-bis{[2-(di-methylamino)ethyl]amino}-4, 8-dihydroxyanthracene-9, 10-dione] was used as counterstain. Scale bar: 50 µm. B, WT metatarsals of embryos at E18.5 were either untreated (n = 17), treated with recombinant murine SPARCL1 (mSPARCL1, 1.5 µg/mL; n = 8), or treated with vascular endothelial growth factor (100 ng/mL; n = 11) alone or in combination with mSPARCL1 (n = 10). Vessel endothelial cells are visualized by CD31 staining. One representative picture of 3 experiments is depicted. Scale bar: 500 µm. Quantification of relative numbers of branches and junctions includes pooled results of all experiments. Error bars indicate SD. *$P < 0.05$ and ****$P < 0.0001$ by 2-tailed, unpaired Student *t* test.

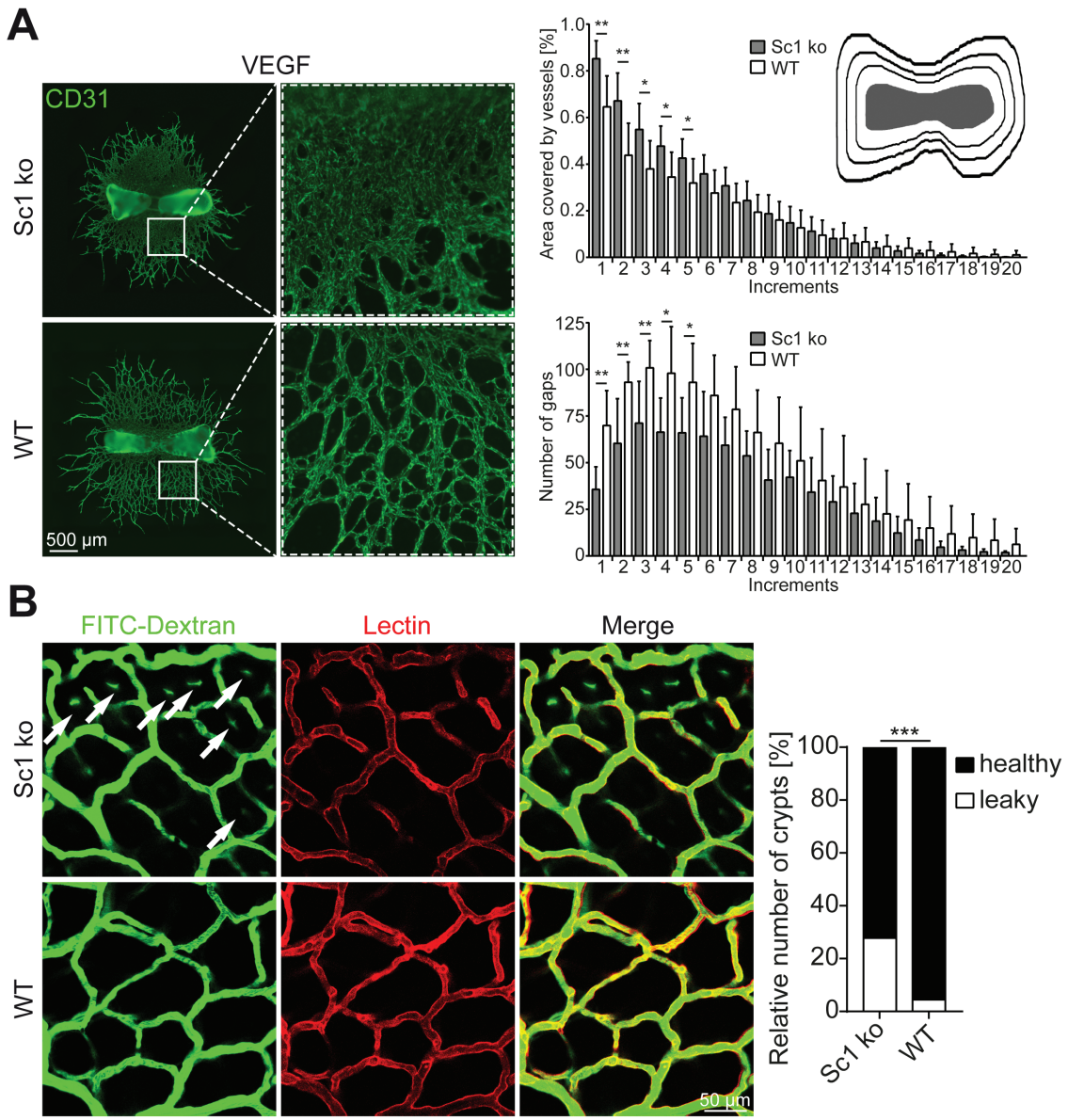

FIGURE 2. SPARCL1 is required for vessel morphogenesis and integrity. A, Sc1 ko (n = 6) and WT (n = 11) metatarsals of embryos at E18.5 were treated with vascular endothelial growth factor (100 ng/mL). Vessel endothelial cells are visualized by CD31 staining, and 1 representative picture is shown. Scale bar: 500 µm. Mean of vessel signal per area and number of intervessel gaps per area were quantified. In total, 20 increments surrounding the bones were defined with an area of 600,000 pixels per increment, starting with increment 1 as the first next to the bone (compare scheme, top right). Error bars indicate SD. *$P < 0.05$, **$P < 0.01$ by 2-tailed unpaired Student t test. B, Sc1 ko (n = 7) and WT (n = 7) mice were subjected to intravital microscopy of the colon. FITC-dextran was used to visualize vessels and the permeability of the crypts through FITC-dextran accumulation inside the crypts (green; examples indicated by arrows). Lectin was used to counterstain vessels only (red). Scale bar: 50 µm. Relative numbers of healthy crypts compared to leaky ones were quantified. In total, 1167 Sc1 ko and 723 WT crypts were counted and evaluated. ***$P < 0.001$ by χ^2 test.

SPARCL1 Deficiency Increases Susceptibility for Acute and Chronic DSS-Induced Colonic Inflammation

A recent study reported that increased vessel permeability contributes to colonic inflammation in DSS colitis in mice and IBD in humans.[18] Accordingly, we hypothesized that Sc1 ko mice may exhibit an increased susceptibility for DSS colitis formation. Therefore, the mice were subjected to 2 different models of colitis (acute and chronic). First, acute colitis was induced by treatment with 2.5% or 2% DSS. The application of standard concentrations of DSS (2.5% and 2%) resulted in rapid weight loss in Sc1 ko mice, requiring the premature termination of experiments (data not shown). Accordingly, a

reduced concentration of DSS had to be used (1.5%) in subsequent experiments in the acute setting (Fig. 3A). The course of disease was monitored by mini-endoscopy, using an endoscopic score based on thickening of the colon wall, changes in the normal vascular pattern, the presence of fibrin, mucosal granularity, and stool consistency according to Becker et al.[26] Sc1 ko mice exhibited significantly increased colonic inflammation as detected by higher endoscopic scores (Fig. 3B).

Next, Sc1 ko and WT mice were subjected to a chronic DSS-induced colitis model with 3 repetitive cycles of a DSS application (Fig. 3A). To prevent an exaggerated course of the disease requiring premature termination of the experiment in many of the mice, the DSS concentration was further reduced to 1%. Under these conditions, 2 WT mice and 4 of the apparently more sensitive Sc1 ko mice still had to be killed because of considerable weight loss (Fig. 3A). Monitoring the endoscopic score after each DSS cycle revealed that after the first cycle, similar to the acute conditions, the endoscopic score was higher in Sc1 ko mice than in the WT mice. After the second and third cycle in both groups of mice, the endoscopic score was very high and did not allow a differentiation of the disease states (Fig. 3A).

The endoscopic score mostly integrates structural changes of the epithelial layer in the colon that in the DSS model arise predominantly during the initial inflammatory response. In a chronic situation, complex structural tissue remodeling occurs that can be resolved in a more suitable manner by histologic scoring. Histologic scoring in the Sc1 ko group under conditions of acute colitis presented a disrupted epithelial barrier but overall only a slightly higher degree of inflammation as compared with the WT group. In contrast, in the chronic colitis group the overall grade of inflammation was significantly increased in the Sc1 ko group as compared with the WT mice (Fig. 3D).

Exaggerated inflammation in the Sc1 ko mice was further supported by an increased detection of fibrosis (Fig. 3D, insert at bottom left image) and the presence of tertiary lymphoid structures (Fig. 3D insert at bottom right image), similar to human chronic disease. In addition, colon length was shorter in Sc1 ko mice than in WT mice in both acute and chronic DSS colitis (Fig. 4A). Moreover, an in vivo analysis of colon vascular leakage with intravital microscopy after intravenous injection of FITC-dextran at the endpoint showed that vascular permeability during acute (Fig. 4B) and chronic (Fig. 4C) DSS colitis was significantly increased in Sc1 ko mice as compared with WT mice.

The AD Is Required for SPARCL1 Anti-Angiogenic Activity

To further validate our results and to provide first mechanistic insights on the effects of SPARCL1, a structure-function analysis of its anti-angiogenic activity was carried out. SPARCL1 consists of a signal peptide regulating the secretion of the protein and 3 different domains, including the AD, the FLD, and the ECBD (Fig. 5A). To investigate which domain may be required for anti-angiogenic activity, mutant proteins with deletions of the different domains were expressed in HeLa cells and purified by His-tag chromatography from the cell culture supernatants. Coomassie staining of the proteins (Fig. 5B) and mass spectrometry (data not shown) confirmed identity, high purity, and correct molecular weights. Human SPARCL1 purified by this approach maintained anti-angiogenic activity in the metatarsal angiogenesis assay; this effect could be neutralized by the addition of a human SPARCL1-specific antibody but not by a nonbinding isotype control antibody (Fig. 5C). These results were confirmed by quantitative analyses of the numbers of branches and junctions (Fig. 5C, right).

SPARCL1 mutants with deleted FLD or ECBD domains maintained their anti-angiogenic activity, whereas this finding was abrogated by the deletion of the acidic domain (Fig. 5D). These results were confirmed by a quantitative evaluation of angiogenic activity, showing that the AD is required for the anti-angiogenic effects of SPARCL1 (Fig. 5D, right).

DISCUSSION

The matricellular protein SPARCL1 was recently described as a novel marker of TME-associated vascular plasticity in CRC.[3] It characterizes quiescent endothelial cells in blood vessels of the normal colon and in CRC tissues with a Th1-like angiostatic tumor microenvironment associated with a favorable prognosis.[3, 15] SPARCL1 harbors an N-terminal signal peptide and is actively released from quiescent endothelial cells via the classical secretion pathway. Soluble purified SPARCL1 has inhibited endothelial cell proliferation and migration in vitro.[3]

Herein, we validated the anti-angiogenic activity of soluble SPARCL1 using the ex vivo mouse metatarsal test.[19] This assay allows the analysis of blood vessel growth that drives the formation of a robust and complex vascular network. In this model, both purified murine and human SPARCL1 (identity protein: 66.8 %; DNA: 74.3 %) inhibited angiogenesis. The anti-angiogenic effect of SPARCL1 was specific because the effect could be abrogated with a specific SPARCL1-neutralizing antibody and by the deletion of the AD of SPARCL1. The anti-angiogenic effect of SPARCL1 was in agreement with the finding that SPARCL1/SPARC double ko mice exhibit increased vessel density during a foreign body response reaction.[27] A putative role of SPARC could be neglected in our experimental setup, first because only purified SPARCL1 protein was used and second because SPARC expression is low or absent in colon tissues.[14] Interestingly, other research has reported that quiescent endothelial cells secrete paracrine-active factors of unknown identity that inhibit the proliferation, invasion, and pro-tumorigenic signaling of lung and breast cancer cells.[28] The coincidences in the expression of and inhibitory effects on

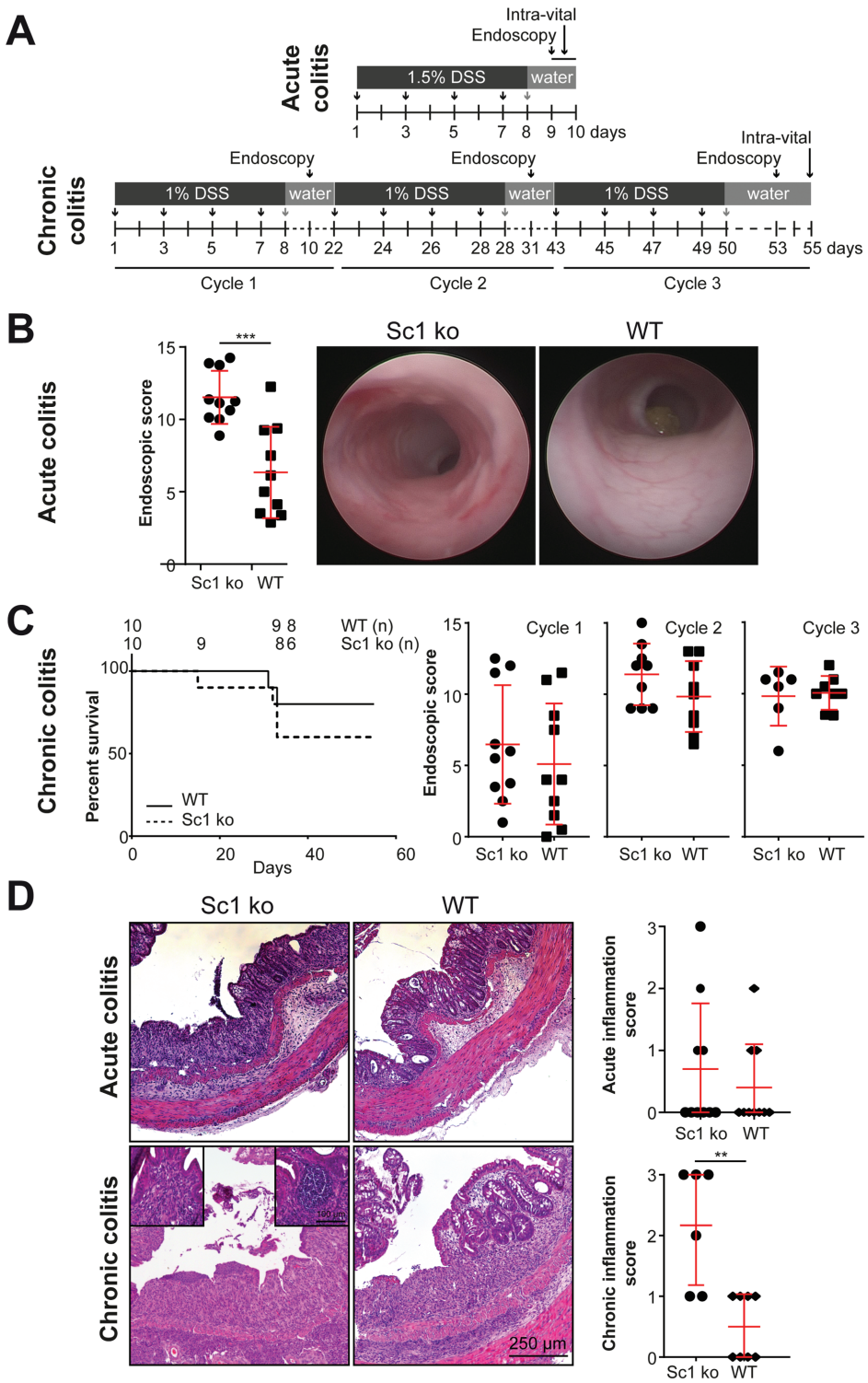

FIGURE 3. *SPARCL1* gene ko promotes acute and chronic DSS-induced colonic inflammation. A, Schematic overview of DSS-induced (acute and chronic) colitis with timepoints of DSS application, endoscopy, and intravital microscopy. The severity of colitis in Sc1 ko (n = 10) and WT (n = 10) mice was evaluated by (B) the endoscopic score in the acute colitis model. C, Survival analysis (left panel) and endoscopic score (right panel) of the Sc1 ko and WT (n=10 each) mice during the chronic colitis model (scores separated for each cycle). D, Histological analysis using H&E staining of the Sc1 ko and WT mice in the acute and chronic colitis model (left panel, scale bar 250 µm). Inserts show fibrosis (left insert) and tertiary lymphoid structures in the chronic model (right insert, scale bar 100 µm). Quantification of the amount of acute and chronic inflammation as detected by H&E staining (right panel). $^{**}P < 0.01$, $^{***}P < 0.001$ by 2-tailed unpaired Student *t* test. H&E indicates hematoxylin-eosin.

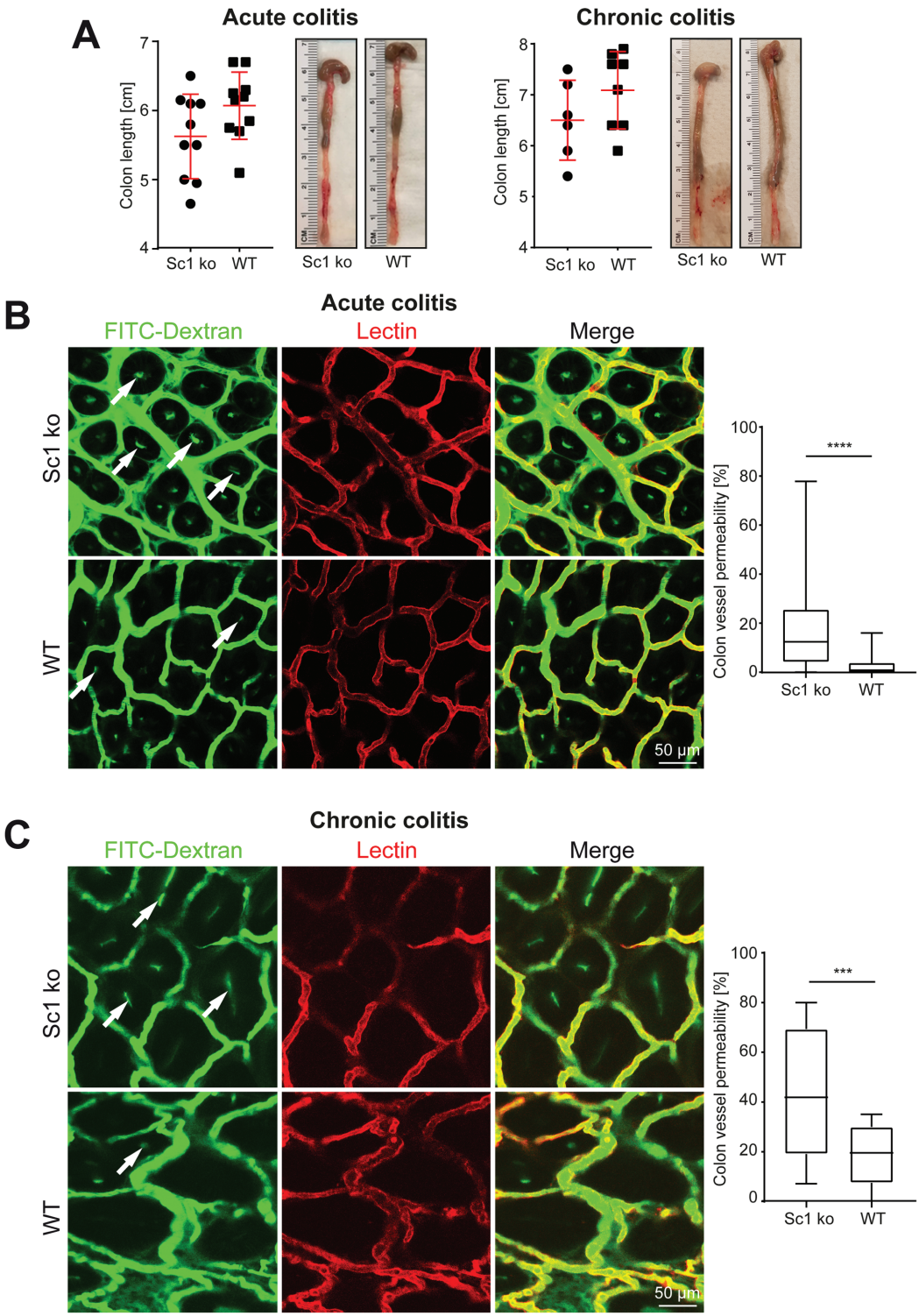

FIGURE 4. *SPARCL1* gene ko causes reduced colon length and increased vessel permeability in DSS-induced colitis. A, Colon length of Sc1 ko and WT mice in acute and chronic colitis. DSS-treated Sc1 ko and WT mice were subjected to intravital confocal microscopy of the colon in (B) an acute (Sc1 ko, n = 10 vs WT, n =9) and (C) a chronic (n = 10 each) colitis model. FITC-dextran was used to visualize permeability of vessels by leakage and thereby accumulation of the dye accumulation inside the crypts (green; examples indicated by arrows). Lectin was used to counterstain vessels (red). Scale bar: 50 µm. B, Colon vessel permeability calculated by the ratio of the FITC signal inside a crypt and the respective total FITC signal of the whole crypt (8 crypts per mouse, all experiments pooled). ****$P < 0.0001$ by 2-tailed unpaired Student *t* test. C, Relative numbers of tight compared to leaky crypts were quantified. In total, 370 Sc1 ko and 340 WT crypts were counted and evaluated. ***$P < 0.001$ by χ^2 test.

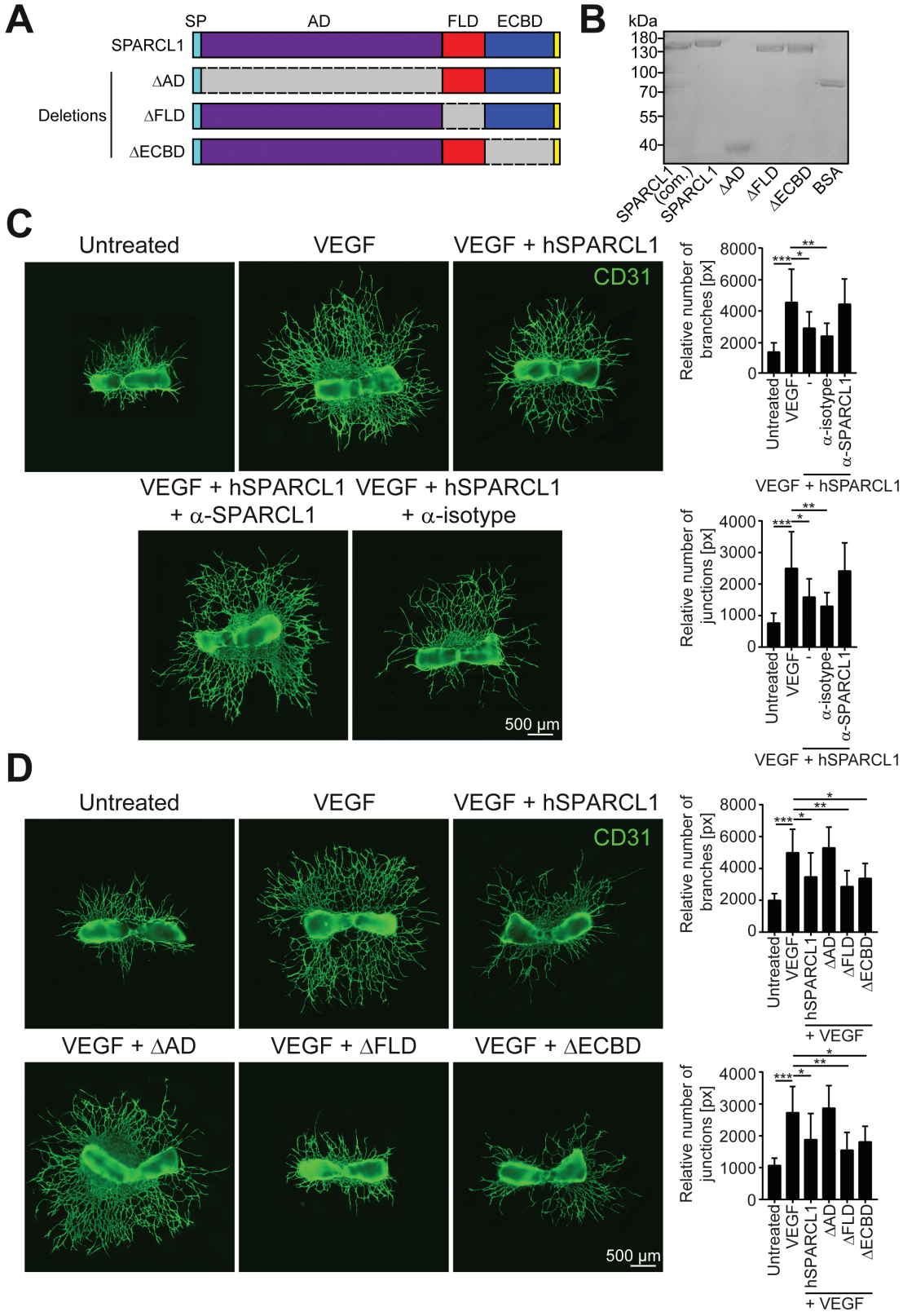

FIGURE 5. The AD of soluble SPARCL1 is required for its anti-angiogenic activity. A, Sc1 WT protein and mutants lacking specific domains of SPARCL1 (ΔAD, ΔFLD, ΔECBD) with a signal peptide for secretion and a Flag-Glycine(9)-His-Tag for purification were expressed in HeLa cells. Secreted proteins were harvested from the cell culture supernatants and subjected to His-Tag chromatography. B, Coomassie stain of FPLC purified proteins

certain tumor cells[16] suggest that SPARCL1 may be considered as contributing to these respective activities.

The ko of the *SPARCL1* gene was associated with increased blood vessel permeability in the mouse colon and morphogenetic alterations of vessels in the metatarsal test. The increased permeability in normal colon vessels occurred in the absence of angiogenic stimulation, indicating that it did not occur because of increased angiogenic activity, which is commonly associated with increased permeability. More likely, increased permeability resulted from a general vessel malformation and/or incomplete maturation. Interestingly, it has been reported that vessels less densely covered with pericytes exhibit a more flattened phenotype and increased diameter, similar to that observed in the vessels of the Sc1 ko mice in our metatarsal test.[29, 30] This finding is also in agreement with the observation that SPARCL1-negative vessels in human CRC tissues with low SPARCL1 expression and in Sc1 ko mice were covered less densely with pericytes and exhibited an increased diameter.[3]

In addition, sprouting from Sc1 ko metatarsals under conditions of angiogenic activation did not result in an increased sprout length as compared with WT mouse metatarsals but did affect the morphology of the sprouts (Fig. 2A). This finding indicates that the primary function of endogenous SPARCL1 is not to counteract angiogenesis under conditions of high angiogenic stimulation, which is in agreement with the finding that SPARCL1 is downregulated under these conditions.[3] In contrast, SPARCL1 likely is required at the end of the sprouting process to stabilize endothelial cell quiescence and vessel maturation and in conditions of low or absent angiogenic stimulation.

The importance of SPARCL1 in the regulation of vessel integrity was further supported by 2 independent experimental mouse models of DSS colitis (acute and chronic). A recent study showed that increased vessel permeability is an important driver of IBD pathogenesis and inflammation, irrespective of the angiogenic activity in the tissues.[18] Interestingly, Sc1 ko mice exhibited a significantly increased susceptibility to DSS-induced colitis, and this was associated with a significantly increased vessel permeability as compared with WT mice.

To identify the domain responsible for the inhibition of angiogenesis, a structure-function analysis of purified SPARCL1 proteins in the metatarsal test was carried out. Using this approach, the AD was found to be necessary for the paracrine angiostatic activity of SPARCL1. The SPARCL1 mutants with deleted FLD or ECBD domains maintained an anti-angiogenic activity similar to the WT protein. Primary sequence alignment of SPARCL1 and its close relative SPARC showed that the amino-terminal AD is the least conserved domain within the SPARC family.[31] Interestingly, synthetic peptides from this region in SPARC have been shown to inhibit endothelial cell spreading, chemotaxis-to-fibroblast growth factor, and the production of fibronectin and thrombospondin 1.[31] All of these results are well in agreement with our observation that the SPARCL1 AD harbors the anti-angiogenic activity of the protein.

CONCLUSIONS

Our study suggests that SPARCL1 not only is a marker of quiescent blood vessels in normal colon tissues and in CRC with a Th1 TME but also functionally contributes to establish the respective plastic phenotype. It inhibits angiogenesis and regulates vessel morphogenesis and integrity. As such, SPARCL1 may be a clinically relevant molecule for diagnostic approaches to determine susceptibility to colitis and for vascular-directed therapy approaches to IBD.

SUPPLEMENTARY DATA

Supplementary data are available at *Inflammatory Bowel Diseases* online.

Supplementary Figure 1. Formation of complex vascular networks in the metatarsal assay. WT metatarsals of embryos E18.5 were treated with vascular endothelial growth factor (100 ng/mL) on days 3, 5, 7 and 9. CD31 (green) was used as an endothelial cell marker, Sm22α (red) was used as a smooth muscle cell marker, and DAPI (blue) was used for the counterstaining of nuclei. Arrows indicate endothelial cells covered with smooth muscle cells.

ACKNOWLEDGMENTS

We thank the Optical Imaging Centre Erlangen (Erlangen, Germany) for excellent support in microscopic techniques. In addition, we gratefully acknowledge the generous help of Uwe Sonnewald and Max Kraner (Division of Biochemistry,

in comparison to a commercially available purified WT SPARCL1 (200 ng each) and body surface area as reference. C, WT metatarsals of embryos at E18.5 were either left untreated (n = 10) or were treated with VEGF (100 ng/mL) (n = 11) alone or in combination with recombinant hSPARCL1 (1.5 µg/mL; n = 11) on days 3, 5, 7, and 9. SPARCL1 neutralization was performed using the hSPARCL1 antibody (α-SPARCL1; n = 10) in a 5-fold molar concentration and the respective isotype antibody (α-isotype; n = 9) as a control. Vessel endothelial cells were stained with CD31. One representative picture of 2 experiments is shown. Quantification of relative numbers of branches and junctions includes pooled results of all experiments. D, Similar to panel C, WT metatarsals were either untreated (n = 6) or treated with VEGF (100 ng/mL; n = 13) either alone or in combination with hSPARCL1 (1.5 µg/mL = 11.1 nM; n = 7), ΔAD (11.1 nM; n = 6), ΔFLD (11.1 nM; n = 5), or ΔECBD (11.1 nM; n = 7). Vessel endothelial cells are visualized by CD31 staining. One representative picture is shown. Relative numbers of branches and junctions are quantified. C and D, Scale bars: 500 µm. Error bars indicate SD. *$P < 0.05$, **$P < 0.01$, ***$P < 0.001$ by 2-tailed unpaired Student *t* test. hSPARCL1 indicates human SPARCL1; VEGF, vascular endothelial growth factor.

Department of Biology, University Erlangen-Nürnberg, Germany) with mass spectrometry and of Thomas Pöschinger (Discovery Oncology, Roche Innovation Center Munich, Penzberg, Germany) for providing Alexa647-labeled lectin and directions for its use. The present work was performed in (partial) fulfillment of the requirements for obtaining the degree Dr. rer. nat. for coauthor Daniela Regensburger.

REFERENCES

1. Goveia J, Rohlenova K, Taverna F, et al. An integrated gene expression landscape profiling approach to identify lung tumor endothelial cell heterogeneity and angiogenic candidates. *Cancer Cell.* 2020;37:421.
2. Carmeliet P. Angiogenesis in health and disease. *Nat Med.* 2003;9:653–660.
3. Naschberger E, Liebl A, Schellerer VS, et al. Matricellular protein SPARCL1 regulates tumor microenvironment-dependent endothelial cell heterogeneity in colorectal carcinoma. *J Clin Invest.* 2016;126:4187–4204.
4. Wang HU, Chen ZF, Anderson DJ. Molecular distinction and angiogenic interaction between embryonic arteries and veins revealed by ephrin-B2 and its receptor Eph-B4. *Cell.* 1998;93:741–753.
5. Adams RH, Wilkinson GA, Weiss C, et al. Roles of ephrinB ligands and EphB receptors in cardiovascular development: demarcation of arterial/venous domains, vascular morphogenesis, and sprouting angiogenesis. *Genes Dev.* 1999;13:295–306.
6. Birke K, Lütjen-Drecoll E, Kerjaschki D, et al. Expression of podoplanin and other lymphatic markers in the human anterior eye segment. *Invest Ophthalmol Vis Sci.* 2010;51:344–354.
7. Marcu R, Choi YJ, Xue J, et al. Human organ-specific endothelial cell heterogeneity. *Iscience.* 2018;4:20–35.
8. Sabbagh MF, Heng JS, Luo C, et al. Transcriptional and epigenomic landscapes of CNS and non-CNS vascular endothelial cells. *Elife* 2018;7:e36187.
9. St Croix B, Rago C, Velculescu V, et al. Genes expressed in human tumor endothelium. *Science.* 2000;289:1197–1202.
10. Savant S, La Porta S, Budnik A, et al. The orphan receptor Tie1 controls angiogenesis and vascular remodeling by differentially regulating Tie2 in Tip and stalk cells. *Cell Rep.* 2015;12:1761–1773.
11. Strasser GA, Kaminker JS, Tessier-Lavigne M. Microarray analysis of retinal endothelial tip cells identifies CXCR4 as a mediator of tip cell morphology and branching. *Blood.* 2010;115:5102–5110.
12. del Toro R, Prahst C, Mathivet T, et al. Identification and functional analysis of endothelial tip cell-enriched genes. *Blood.* 2010;116:4025–4033.
13. Bradshaw AD. Diverse biological functions of the SPARC family of proteins. *Int J Biochem Cell Biol.* 2012;44:480–488.
14. Girard JP, Springer TA. Cloning from purified high endothelial venule cells of hevin, a close relative of the antiadhesive extracellular matrix protein SPARC. *Immunity.* 1995;2:113–123.
15. Naschberger E, Croner RS, Merkel S, et al. Angiostatic immune reaction in colorectal carcinoma: impact on survival and perspectives for antiangiogenic therapy. *Int J Cancer.* 2008;123:2120–2129.
16. Hu H, Zhang H, Ge W, et al. Secreted protein acidic and rich in cysteine-like 1 suppresses aggressiveness and predicts better survival in colorectal cancers. *Clin Cancer Res.* 2012;18:5438–5448.
17. Haep L, Britzen-Laurent N, Weber TG, et al. Interferon gamma counteracts the angiogenic switch and induces vascular permeability in dextran sulfate sodium colitis in mice. *Inflamm Bowel Dis.* 2015;21:2360–2371.
18. Langer V, Vivi E, Regensburger D, et al. IFN-γ drives inflammatory bowel disease pathogenesis through VE-cadherin-directed vascular barrier disruption. *J Clin Invest.* 2019;129:4691–4707.
19. Song W, Fhu CW, Ang KH, et al. The fetal mouse metatarsal bone explant as a model of angiogenesis. *Nat Protoc.* 2015;10:1459–1473.
20. Schindelin J, Arganda-Carreras I, Frise E, et al. Fiji: an open-source platform for biological-image analysis. *Nat Methods.* 2012;9:676–682.
21. Naschberger E, Geißdörfer W, Bogdan C, et al. Processing and secretion of guanylate binding protein-1 depend on inflammatory caspase activity. *J Cell Mol Med.* 2017;21:1954–1966.
22. Hohenester E, Maurer P, Timpl R. Crystal structure of a pair of follistatin-like and EF-hand calcium-binding domains in BM-40. *Embo J.* 1997;16:3778–3786.
23. Tripal P, Bauer M, Naschberger E, et al. Unique features of different members of the human guanylate-binding protein family. *J Interferon Cytokine Res.* 2007;27:44–52.
24. Naschberger E, Lubeseder-Martellato C, Meyer N, et al. Human guanylate binding protein-1 is a secreted GTPase present in increased concentrations in the cerebrospinal fluid of patients with bacterial meningitis. *Am J Pathol.* 2006;169:1088–1099.
25. McKinnon PJ, McLaughlin SK, Kapsetaki M, et al. Extracellular matrix-associated protein Sc1 is not essential for mouse development. *Mol Cell Biol.* 2000;20:656–660.
26. Becker C, Fantini MC, Neurath MF. High resolution colonoscopy in live mice. *Nat Protoc.* 2006;1:2900–2904.
27. Barker TH, Framson P, Puolakkainen PA, et al. Matricellular homologs in the foreign body response: hevin suppresses inflammation, but hevin and SPARC together diminish angiogenesis. *Am J Pathol.* 2005;166:923–933.
28. Franses JW, Baker AB, Chitalia VC, et al. Stromal endothelial cells directly influence cancer progression. *Sci Transl Med.* 2011;3:66ra5.
29. Eilken HM, Diéguez-Hurtado R, Schmidt I, et al. Pericytes regulate VEGF-induced endothelial sprouting through VEGFR1. *Nat Commun.* 2017;8:1574.
30. Hellström M, Gerhardt H, Kalén M, et al. Lack of pericytes leads to endothelial hyperplasia and abnormal vascular morphogenesis. *J Cell Biol.* 2001;153:543–553.
31. Sullivan MM, Sage EH. Hevin/SC1, a matricellular glycoprotein and potential tumor-suppressor of the SPARC/BM-40/osteonectin family. *Int J Biochem Cell Biol.* 2004;36:991–996.